# Trace element distribution, solid- and fluid inclusions in untreated Mong Hsu rubies

**Florian Mittermayr[1,2], Jürgen Konzett[2], Christoph Hauzenberger[3], Reinhard Kaindl[2] & AlexanderSchmiderer[4]**

[1]Department of Applied Geosciences, Graz University of Technology, Rechbauerstraße 12, 8010 Graz, Austria (e-mail: f.mittermayr@tugraz.at)
[2]Institute of Mineralogy and Petrography, Leopold-Franzens University Innsbruck, Innrain 52, 6020 Innsbruck, Austria
[3]Institute of Earth Sciences, Department of Mineralogy and Petrology, Universitätsplatz 2, 8010 Graz, Austria
[4]Curt Engelhorn Centre for Archaeometry, 68159 Mannheim, Germany

## 1. Introduction

Mong Hsu/Myanmar has been an important source for gem quality ruby since the early 1990's. White calcite-dolomite marbles are the host rock for well developed crystals that are thought to have formed at amphibolite facies conditions of 500-550C° and 2.0-2.5kbar (Peretti et al. 1996). The most apparent characteristic of untreated Mong Hsu rubies is a distinctive optical zoning whereby a dark blue to black sapphire core is surrounded by a red ruby rim. More complex zoning patterns such as oscillatory color zoning may also be present. The association of optical with chemical zoning has already been discussed in several studies (e.g. Achiwawanich et al. 2006) and was related to a zonal distribution of Cr, Ti, V and Fe. Nevertheless, additional knowledge of the trace element contents is fundamental to understanding the unique optical appearance of Mong Hsu rubies. Aside from minor/trace element patterns, solid and fluid inclusions are an additional important feature that can be used to identify specific corundum deposits and to distinguish between natural and synthetic corundum. In case of Mong Hsu rubies, liquid $CO_2$-inclusions and a suite of solid inclusions involving diaspore, white mica, rutile and dolomite are typical (Peretti et al. 1995).

The aim of this study is to gain better insight into the color zoning mechanisms and formation conditions of the Mong Hsu rubies by investigating their minor and trace element zoning patterns as well as fluid and solid inclusions and to compare these data with those already available from the literature.

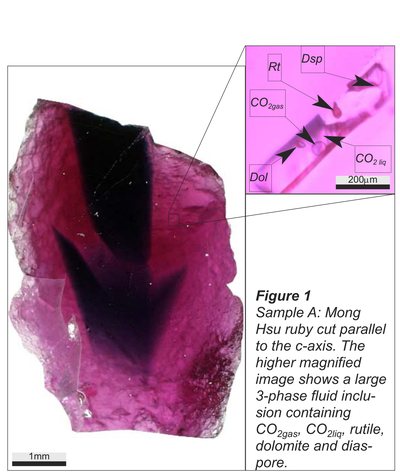


***Figure 1***
*Sample A: Mong Hsu ruby cut parallel to the c-axis. The higher magnified image shows a large 3-phase fluid inclusion containing $CO_{2gas}$, $CO_{2liq}$, rutile, dolomite and diaspore.*

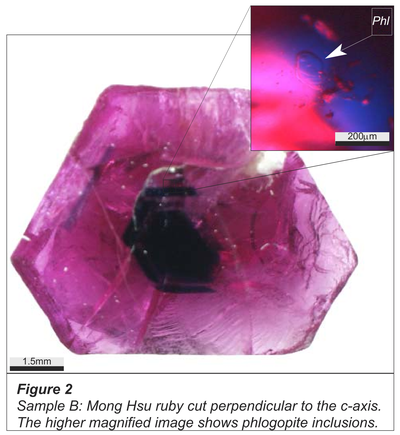


***Figure 2***
*Sample B: Mong Hsu ruby cut perpendicular to the c-axis. The higher magnified image shows phlogopite inclusions.*

## 2. Sample Material and Analytical Methods

Three transparent samples (diameter 0.5 cm) with black sapphire cores und ruby rims and a number of smaller and less transparent specimens (diameter 0.1 cm) were investigated. Two of the larger samples are displayed: Sample A is cut parallel to the crystallographic c-axis (figure 1); Sample B is cut perpendicular to the c-axis (figure 2). Optical zoning and the position of solid and fluid inclusions were located with optical microscopy. Chemical zoning was then investigated with backscattered electron imaging (BSE) (figure 3) and cold cathodoluminescence imaging (CL) (figure 4). Spot analyses and element distribution mappings of Cr and Ti were performed using the electron microprobe (EMP) (Figure 5 ). Trace element contents were measured using Laser Ablation ICP-MS. (LA-ICP-MS). This method offers very low detection limits (< 1 ppm, use of collision-cell technology) combined with a spatial resolution as low as 10 µm. We used a Thermo Elemental XSeries II Quadrupol-ICP-MS coupled with a Merchantek 213 nm Laser. The ablation gas was Helium. The results are fully quantitative using the liquid calibration according to Halicz and Günther (2004). When comparable, WDX analyses are in excellent agreement with LA-ICP-MS data. In addition to the mineral chemical study, laser Raman spectroscopy was used to identify fluid, gas solid inclusions.

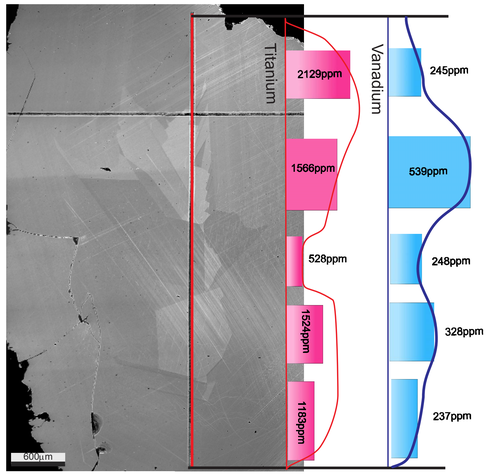


***Figure 3***
*BSE image of Sample A with an overlay illustrating the distribution of the elements Ti and V.*

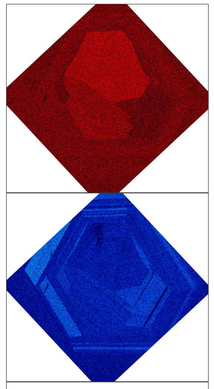

***Figure 5***
*Element distribution images of Cr in upper and Ti in the lower figure of sample B. Lighter colors indicate a higher concentration as darker ones. Values ranging from 4000-7500ppm for Cr and from 500-2000ppm for Ti.*

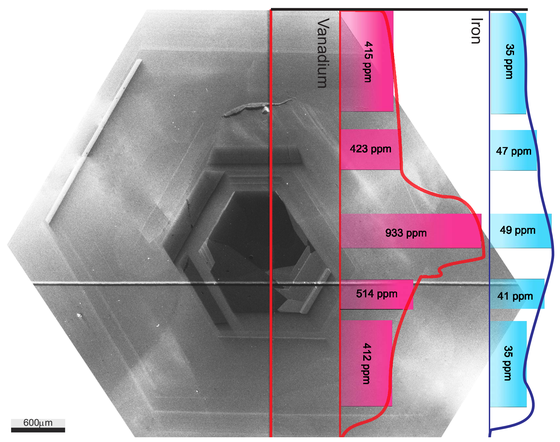


***Figure 4***
*CL image of Sample B with an overlay illustrating the distribution of the elements Fe and V.*

| Element | l.o.d. (ppm) | Sample A Core (ppm) | Sample A Rim ppm) | Sample B Core (ppm) | Sample B Rim (ppm) | All samples range (ppm) | Median (ppm) | Analysis (n) |
|---|---|---|---|---|---|---|---|---|
| Mg | 0,2 | 74,7 | 16,3 | 89,2 | 28,6 | 16.3-89.2 | 51,6 | 4 |
| Ti | 1,2 | 1566,1 | 1183,3 | 1865,2 | 1215,9 | 528.4-2520.6 | 1222,9 | 33 |
| V | 0,4 | 538,9 | 244,9 | 933,3 | 399,5 | 236.6-933.3 | 255,1 | 33 |
| Cr | 0,2 | 14768,8 | 7514,5 | 7079,3 | 3553,8 | 2684.5-14768.8 | 4426,9 | 33 |
| Fe | 0,3 | 90,1 | 59,3 | 49,2 | 35,1 | 28.1-90.1 | 61,4 | 33 |
| Cu | <0,1 | 0,2 | 0,2 | 0,3 | 0,2 | <0,1-1.5 | 0,2 | 33 |
| Zn | <0,1 | 0,3 | 0,4 | 0,5 | 0,6 | <0,1-2.4 | 0,4 | 33 |
| Ga | <0,1 | 41,6 | 36,7 | 56,6 | 49,2 | 35.7-56.6 | 48,1 | 33 |
| As | <0,1 | 0,8 | 0,6 | 0,5 | 0,6 | 0.3-1.1 | 0,6 | 33 |
| Nb | <0,1 | 2,1 | <0,1 | 4,1 | <0,1 | <0,1-4.1 | <0,1 | 33 |
| Ta | <0,1 | 1,3 | <0,1 | 0,6 | <0,1 | <0,1-1.3 | <0,1 | 33 |
| W | <0,1 | 46,0 | <0,1 | 49,3 | <0,1 | <0,1-49.3 | <0,1 | 33 |
| Th | <0,1 | 0,3 | <0,1 | 0,3 | <0,1 | <0,1-0.4 | <0,1 | 33 |

***Table 1***
*Chemical composition of Mong Hsu rubies measured by LA-ICP-MS. Values given in ppm.*

## 3. Results & Discussion

Mong Hsu rubies show a very complex zoning of a suite of minor and trace elements that are partially linked to their optical color zoning. Dark blue to black inner cores show elevated concentrations of Cr, V, Mg, Nb, Ta, W and Th compared to the outer rims. Fe, which is considered by various authors (e.g. Peretti et al. 1995) to be the activator of color zoning is only slightly enriched in the inner dark cores and shows no further distinctive distribution patterns. Blue interlayer zones surrounding the cores (sample B figure 2) do not show any enrichment in Fe but do show a significant enrichment in Ti. Ga, Cu, Zn and As are homogeneously distributed throughout the samples. Extremely high Cu concentrations (145-756ppm) described by Osipowicz et al. (1995) could not be verified as measured Cu values are in the range of 0.2 ppm (cf. Table 1). By plotting Cr/Ga vs. Fe/(V+Ti) Mong Hsu rubies can be distinguished from rubies found in other localities (figure 5).

We suggest that formation conditions of Mong Hsu rubies are significantly higher than 500-550°C and 2.0-2.5 kbar as previously reported by Peretti et al. (1996). EPM spot analysis of the Zr-contents of 5 different rutile inclusions in one sample where performed using the analytical procedure described in Zack et al. (2004). Application of the Zr-in-rutile thermometer calibration by Ferry and Watson (2007) yields the following temperatures: Rt1 (215 ppm Zr) 617+/-40°C, Rt2 (230 ppm Zr) 622+/-40°C, Rt3 (511 ppm Zr) 688+/-45°C, Rt4 (193 ppm Zr) 609+/-40°C, Rt5 (267 ppm Zr) 634+/-40°C indicating upper amphibolite facies metamorphic conditions. Due to regional metamorphism as described by Tin Hlaing (1993) it is further suggested that pressures are in the range of 4-6kbar. Conditions of 500-550°C and 2.0-2.5 kbar proposed by Peretti et al. (1996) may thus reflect retrograde metamorphism with attendant late hydrothermal activity responsible for abundant fluid inclusions lining healed fissures.

Using laser Raman spectroscopy a suite of solid inclusions involving Cr-muscovite, paragonite-margarite solid solutions, phlogopite, Mg-rich chlorite, rutile, quartz, dolomite and diaspore were identified (figure 2). The latter four phases have also been identified in fluid inclusions containing $CO_2$ as only liquid, most likely representing daughter crystals that have formed from an originally mixed $CO_2$-$H_2O$ fluid (figure 1). After heating by the light of the microscope larger fluid inclusions exsolve bubbles of $CO_2$ gas. In one fluid inclusion $H_2S$ and $CO_2$ was detected.

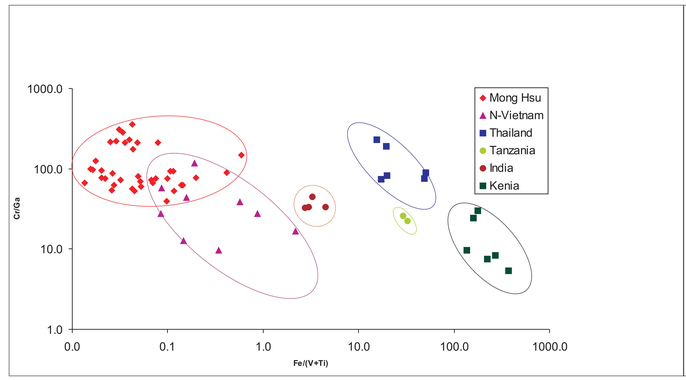


***Figure 5***
*Chemical diagram Cr/Ga vs. Fe/(Ti+V) of Mong Hsu rubies and rubies from different geological origins.*

**4. Acknowledgement**

The authors wish to thank D. Swarovski & Co. for suppling sample material.

**5. References**

Achiwawanich S. et al. (2006) Applied Surface Science, Vol. 252, No. 24, 8646-8650.
Ferry J.M. and Watson E.B. (2007) Contrib. Mineral. Petrol., Vol. 154, 429-437.
Halicz L. and Günther D. (2004) J. Anal. At. Spectrom., Vol. 19, 1539-1545.
Osipowicz T. et al. (1995) Nuclear Instruments and Methods in Physics Research, Vol. 104, 590-594.
Tin Hlaing (1993) Austr. Gemmol., Vol. 18, 157-160.
Peretti A. et al. (1995) Gems & Gemology, Vol. 31, No. 1, 2-26.
Peretti A. et al. (1996) Journal of Gemmology, Vol. 25, No. 1, 3-19.
Zack T. et al. (2004) Sedimentary Geology, Vol. 171, No. 1-4, 37-58.